Analytical Methods

Accepted Manuscript

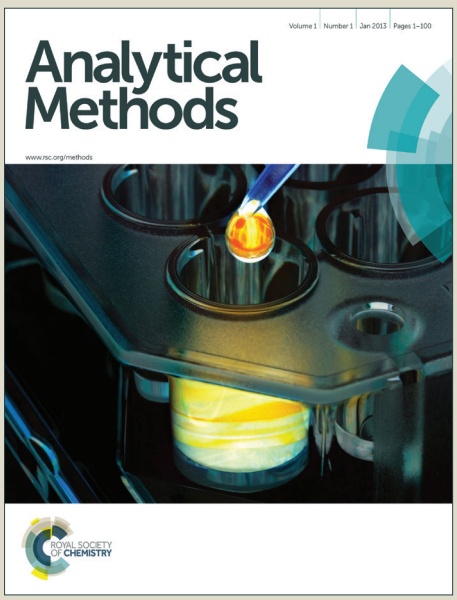

ROYAL SOCIETY OF CHEMISTRY

www.rsc.org/methods

Electrochemical Response of Agar Ionogels towards Glucose Detection

Anshu Sharma[1, 2], Kamla Rawat[2*], Pratima R. Solanki[2*] and H. B. Bohidar[1, 2]

[1]School of Physical Sciences, Jawaharlal Nehru University, New Delhi, India
[2]Special Centre for Nanoscience, Jawaharlal Nehru University, New Delhi, India
Corresponding authors email: pratimarsolanki@gmail.com; kamla.jnu@gmail.com Tel: +91 11 2670 4740, Fax: +91 11 2674 1837

ABSTRACT

We have reported a sensing platform comprising of agar ionogel (IGs) made in ionic liquid solutions (1-octyl-3-methyl imidazolium chloride [C8mim][Cl] and 1-ethyl-3-methyl imidazolium chloride [C2mim][Cl]) and used it for glucose oxidase (GOx) immobilization for glucose detection. The ionogels were deposited onto indium tin oxide (ITO) coated glass plate using the drop casting technique. These Agar-[C8mim][Cl]/ITO (Ag-C8/ITO) and Agar-[C2mim][Cl]/ITO (Ag-C2/ITO) substrates were used for immobilization of GOx, which was selected as a model enzyme to investigate its interaction with these electrodes using electrochemical techniques. Structural and morphological studies of these GOx/Ag-C8/ITO and GOx/Ag-C2/ITO electrodes were characterized by scanning electron microscopy (SEM), Fourier transform infrared spectroscopy (FTIR) and electrochemical techniques (CV). These GOx/Ag-C8/ITO and GOx/Ag-C2/ITO bioelectrodes exhibited improved glucose detection capability in the concentration range of 0.27- 16.7 mM and 0.28-5.6 mM with sensitivity ≈ 4.1μA mM^{-1}/cm^{-2} and 14.6 μA $mM^{-1}cm^{-2}$, respectively. The value of apparent Michaelis–Menten constant (K_m) was 0.023 mM and 0.0007 mM for the aforesaid two cases respectively. It is shown that, customization of agar hydrogels in green solvent medium widens the scope of its potential applications as glucose sensing in real samples.

Keywords: Agar ionogels, ionic liquid, glucose sensor, electrochemistry.

Introduction

Recently, ionic liquids (ILs) have received much attention as materials with enormous practical applications because of their unique properties that include exceptional ionic conductivity, biocompatibility, electrochemical, thermal stability and non-flammability making them particularly attractive in the development of electrochemical biodevices with long-term stability. As variability in their application potential arises from the availability of a range of ILs molecules with various combinations of anions, cations, hydrophilic head groups, and hydrophobic chain lengths [1-6]. It has been adequately realized that ILs are the green solvents of the future. The novel and remarkable attributes of ILs can be realized from the following facts:(i) ILs can dissolve cellulose [7], (ii) maintain biological activity of DNA in solutions over an extended period [8] and (iii) inhibit pH dependent aggregation of proteins [9]. Moreover ionic liquids are room-temperature molten salts that are increasingly used in electrochemical devices, such as in batteries, fuel cells, and biosensors [10].

The ILs has been used for the different biosensing application because ILs increases the stability of biomolecules and also improves the sensitivity and response time of biosensor [11-12]. ILs is being used for development of different electrochemical biosensor for clinical diagnosis including glucose detection. Liu et al. have reported hydrolysis of tetraethyl orthosilicate in 1-butyl-3-methylimidazolium tetra-fluoroborate (BMIMBF4) based hydrogen peroxide electrochemical biosensor [13]. They have reported that in BMIMBF4, IL improved the film quality without forming any crack in film and also showed improved stability of horseradish peroxidase. An ionic liquid-carbon composite based biosensor has developed using *n*-octyl-pyridinium hexafluorophosphate mixed with graphite powder and glucose oxidase (GOx) for the detection of glucose [14]. Wang et al., [15] studied the electric property of IL (1-Ethyl-3-methylimidazolium Bromide) and single-wall carbon nanotubes, composite material and used this material for immobilizing GOx for glucose detection. Prussian blue modified carbon ionic liquid electrodes (PB-CILEs) fabricated and immobilized GOx on PB-CILE surface using three different procedures involving cross linking with glutaraldehyde, bovine serum albumin and nafion matrix [16]. A multiwalled-carbon nanotubes (MWNTs), gold nanoparticles (AuNPs), chitosan (CS) and room temperature ionic liquid (RTIL) found linearity as 1-10 mM for glucose [17]. Lee et al., fabricated Au-poly $[C_{10}VIm^{+}][Cl^{-}]$ based sensing platform prepared by

combination of IL monomer, 1-decyl-3-vinylimidazolium chloride, [$C_{10}VIm^{+}Cl^{-}$] with an aqueous solution of $HAuCl_4$ and results reported the detection range from 50-100 mM of glucose, which is beyond the physiological range [18]. Recently, Ozokur et al., fabricated a glassy carbon electrode modified with manganese oxide decorated with platinum nanoparticles and monitored bio-catalytic activity of pyranose oxidase bridged by ILs unit [19]. Lourenco et al 2011 studied the effect of different ILs 1-ethyl-3-methyl-imidazolium ethyl sulphate, 1-butyl-3-methyl-imidazolium dycianamide and 1-butyl-3-methyl-imidazolium chloride, 1-butyl-3-methyl-imidazolium tetrafluoroborate, gelatin and water on the activity of GOx and horse redish peroxidise [20]. Thus, there is wide scope for development of electrochemical biosensor using biopolymer and ILs for glucose sensor.

In this work, we have proposed a combined agar and ILs based sensing platform that utilized for electrochemical applications like sensors. Electrochemical technique is a cost effective, simple and fast method of detection of analytes at low concentration [21]. Here, we studied the electrochemical behavior of agar dispersed in two homologous IL solutions i.e. [C2mim][Cl], and [C8mim][Cl] using an array of experimental methods for potential glucose sensing. It found that agar is a very promising candidate for application in electrochemical devices like biosensor, tissue regeneration and drug delivery etc. due to its biocompatibility, good film forming ability, higher stability, high mechanical rigidity and negligible level of cytotoxicity [22-24]. Agar is a phycocolloid, a water soluble polysaccharide, extracted from a group of red marine algae (Class Rhodophyceae) including Gelidium, Pterocladia, Gracilaria and Gelidiella spp. Agar is composed of two principal components e.g. agarose and agaropectin. Agarose is the gelling component, whereas the agaropectin has a low gelling ability. Agar comprises mainly of alternating β-(1-4)-D and α-(1-4)-L linked galactose residues in a way that most of α-(1-4) residues are modified by the presence of a 3,6 anhydro bridge [25-28]. The physical properties of customised agar with ILs are extensively studied in the past [29-30]. Agar, could be an excellent polyanionic biopolymer, is extensively studied due to its gelling ability at low concentration [31-33]. It is expected that the ion mobility in these matrices could be fast due to presence of chloride ions. The [C4mim][Cl] is miscible with silk, and is an attractive biomaterial with excellent mechanical properties and biocompatibility [13]. Moreover, it could provide strong binding affinity towards the biomolecules including enzymes due to availability of abundant hydroxyl groups. Agar in the ILs (ionogels) formed a network *via* strong hydrogen bonds that provides a

microenvironment favorable to biomolecule stability and functionality which is most important aspects for biosensors. It was observed from literature that the optimization of agar in [C2mim][Cl] and [C8mim[[Cl] IL solutions and their application in clinical diagnostic as a biosensing platform has not been explored. Thus, there is wide scope for investigation of agar in ionogel as potential clinical diagnostic biosensing platform. Keeping these point in view, efforts have been made to fabricate an electrode comprising of agar in [C2mim][Cl], and [C8mim][Cl] for embedment of model enzyme, GOx, which is stable and inexpensive enzyme which catalyzes glucose.

In the present work, we have proposed a very simple, easy fabrication, low cost and more stable biosensing electrode fabricated by using of ILs and biopolymer agar. A thin film of uniformly dispersed agar ionogel using [Ag C2 and Ag C8] was prepared on indium tin oxide (ITO) coated glass substrate and utilized for immobilization of GOx for glucose detection. It has been found that Ag C2 and Ag C8 provide improved electrochemical properties including charge transfer rate constant, diffusion coefficient, electroactive surface area and average surface concentration which facilitate to improve the linear detection range and higher affinity for glucose detection.

II. Materials and Methods

Materials and Reagents: Agar was a gift from Central Salt and Marine Research Institute, Bhavnagar, Gujrat. It was extracted from the red seaweed Gracilariadura collected from the Gulf of Mannar off the southeast coast of India, employing a method described in reference [34].The ionic liquid (IL) 1-ethyl-3-methylimidazolium chloride(C2mim[Cl]) and 1-octyl-3-methyl imidazolium chloride [C8mim][Cl], glucose oxidase (GOx) and glucose were brought from Sigma-Aldrich, USA were used as received. All these chemicals were used to prepare solutions in deionized water without further purification. Indium-tin-oxide (ITO) coated glass plates were obtained from Balzers, UK, (Baltracom 247 ITO, 1.1 mm thick) with a sheet resistance and transmittance of 25 Ω $sq^{-1}$and 90%, respectively. Different concentration of glucose was prepared from freshly prepared stock solution (20 mM) of glucose in DI water and stored in refrigerator (4 ^{0}C). Deionized water from Organo Biotech Laboratories, India, was used to prepare the solutions. Six solutions of water (100-x)- IL (x) binary mixture were prepared with concentration of IL (x) (%w/v) varying from 0 to 5%. The biopolymer solutions were prepared by autoclaving the agar powder in required IL-water mixture at 120^{0}C and under high pressure

with concentrations of 0.25% (w/v) of agar and these were homogenized for 10 minutes by stirring while hot. A trace quantity of sodium azide (NaN_3) was added to the samples to prevent bacterial contamination.

Preparation of Ag-C8/ITO and Ag-C2/ITO electrode: Prior to electrode fabrication the biopolymer agar solution was prepared. The agar solution was prepared by dissolving agar powder 0.25% (w/v) in the required [C2mim][Cl] and [C8mim][Cl] (ILs) solutions (optimized concentration) and these were allowed to homogenize by resorting to continuous stirring for 30 minutes at 50^0C. Finally, the Ag-C8/ITO and Ag-C2/ITO bioelectrodes were prepared by drop casting method. Typically, 10 µl of hot sol was spread uniformly onto an ITO surface (0.25 cm^2) and it was allowed to cool to room temperature and form a gel film. These electrodes were stored for about 48 h in an air tight dessicator at room temperature (relative humidity < 50 %) to attain homogeneity. In the next step these films were washed with deionized water to remove any unbound particles and stored in refrigerator (4 ^{0}C) when not in use. The thickness of Ag-C8/ITO and Ag-C2/ITO electrode was found about as 25±2 nm as obtained from ellipsometry (SOPRA cysostat serial-61H2210109) and sensing area was about 0.25 cm^2.

Immobilization of glucose oxidase (GOx) on electrodes: Fresh solution of GOx (2mg mL^{-1}) was prepared in phosphate buffer (50 mM, pH 7.0) and 10 µL solution of freshly prepared GOx was mechanically spread onto the previously prepared Ag-C8/ITO and Ag-C2/ITO electrodes. Binding of enzyme to Ag-C8/ITO and Ag-C2/ITO electrode is facilitated by the electrostatic interaction between amine groups of GOx and hydroxyl group of polyanionic in agar. Generally GOx contains two molecules of flavin adenine dinucleotide (FAD), which efficiently catalyzes the oxidation of glucose generating hydrogen peroxide (H_2O_2). We have followed a common method for the immobilization of water-soluble enzymes on solid substrates, such as an electrode, is through simple electrostatic interaction between oppositely charged species. This approach, while not permitting precise control of protein orientation, is extremely simple, offering facile construction. Electrostatic immobilization of GOx onto Ag-C8/ITO and Ag-C2/ITO electrodes was achieved by addition of GOx (in PB 50 mM, pH 7.0) onto electrodes and kept for 4 h at room temperature (20 ^{0}C) in a humid chamber. These bioelectrode gently rinsed with phosphate buffer to remove any unbound enzymes from the electrode surface and it was

stored in refrigerator (4^0C) when not in use. It was found that bioelectrodes showed highest electrocatalytic behaviour in phosphate buffer at pH 7.

Characterization: Fourier transform infrared (FTIR) spectroscopy studies were carried out using Perkin Elmer, Spectrum BX II and scanning electron microscopy (SEM) by Lvo 40 Zeiss instrument. The surface thickness studies were conducted by Elipsometer: WinElli II any software of Sopra. Electrochemical studies [electrochemical impedance spectroscopy (EIS), cyclic voltammetry (CV)] were conducted on an Autolab Potentiostat/Galvanostat (Eco Chemie, Netherlands) using a three-electrode cell, platinum (Pt) wire as the auxiliary electrode, Ag/AgCl as reference electrode and GOx/Ag-C8/ITO; GOx/Ag-C2/ITO as working electrode in phosphate buffer saline (PBS, pH 7.0,0.9% NaCl) containing 3.3 mM $[Fe(CN)_6]^{3-/4-}$ as redox probe and these three electrodes connected with the potentiostat during electrochemical measurements.

III. Results and Discussion

Ionogel Formation

The ionogel was formed by interaction between agar, and [C2mim][Cl] and [C8mim][Cl] solutions. Addition of ILs to water introduces counter ion (Cl^-), hydrophobicity (C2 and C8) and hydrogen bond forming capability (water with immidozolium head group). The interaction between OH (derived from agar) and IL (both cation and anion) in different circumstances has been confirmed by FT-IR spectroscopy.

Spectroscopic Studies

The surface morphology of (a) Ag-C8/ITO, (b) GOx/Ag-C8/ITO, (c) Ag-C2/ITO and (d) GOx/Ag-C2/ITO bioelectrodes was monitored using scanning electron microscope (SEM). (Fig.1). Image (a) and (c) exhibit the good uniformity and homogeneity without any phase separation, indicating that excellent miscibility occurred between agar and ILs which create a smooth surface. It is clearly seen in image (b) and (d) that the surface morphology of Ag-C8/ITO and Ag-C2/ITO electrode is completely changed after the immobilization of GOx. The honey comb structured formed after the immobilization of GOx onto Ag-C8/ITO electrode (image b). However, the appearance of globular shaped morphology with branched shaped confirmed the binding of GOx onto these electrodes as shown in inset (image d).

Figure 1

Figure 2. depicts the FTIR spectra of (a) Ag/ITO, (b) Ag-C2/ITO, (c)Ag-C8/ITO, (d) GOx/Ag-C8/ITO bioelectrode (in the range of 400-4000 cm^{-1}) to identify the structural and conformational changes based on comparison of absolute peak intensities. The peak at 1080 cm^{-1}, responsible for the vibrational modes of -OH groups and the C-O stretching, may be arising due to skeletal stretches (curve a). A significant change was observed in the FTIR spectra after the addition of ILs to water. The broad IR band appeared at 3426 cm^{-1} was attributed to the OH (hydroxyl groups) stretching of agar (curve a). Drastic change and shift towards occurred towards lower wave number in OH stretching (3426 cm^{-1}) of agar after the addition of ILs. This is attributed to inter-and intramolecular hydrogen bonds formation in (curve b and c). The IR peak at 1566 cm^{-1}, was due to C=C stretch of imidazolium ring present in ILs. The peak at 1460 cm^{-1} was due to symmetrical deformation of CH_3 and CH_2 group, similar peak was also present in Ag-C8/ITO electrode sample due to presence of CH_3 group of ILs (curve b and c). The IR bands near 1180 cm^{-1} can be assigned to C–O–C from agar dissolved in the 1-ethyl-3-methylimidazolium chloride (curve b) and IR band at 1165 cm^{-1} was due to ring in-plane assymetric stretching, C–C and (N) CH_2 stretching (curve c). Other bands near 980 cm^{-1} can be assigned to C–C stretching from agar structure ring and at 790 cm^{-1} to ILs ring HC=CH symmetric bending (curve c). All these changes in IR bands indicated that uniform interaction between the agar and ILs via hydrogen bond and electrostatic interaction between the polyanionic group of agar and amphiphilic nature of ILs. Significant changes which appear after the immobilization of GOx onto Ag-C2/ITO and Ag-C8/ITO electrode was in the region 1000-1800 cm^{-1} as it became broader suggesting that the interaction between amino and hydroxyl group present in Ag-C2/ITO and Ag-C8/ITO electrode. The intensity of IR peak becomes higher and broader due to presence of functional groups of GOx corresponding to amide I (1640 cm^{-1}) and amide II (1560 cm^{-1}), respectively, indicating immobilization of GOx onto this matrix (curve d).

Figure 2

Electrochemical Studies

The electrochemical behaviour of electrodes, containing ILs of different concentration varying from 1.0-5.0 % (w/v), were optimized using cyclic voltammetry (CV) at scan rate of 20

mV/s in PBS containing 3.3 mM$[Fe(CN)_6]^{3-/4-}$ [inset, Fig. 3(A)]. It was observed that the magnitude of current maxima was obtained at [IL] =2% (w/v) for Ag-C8/ITO, and at [IL] =4% (w/v) for Ag-C2/ITO electrode, which indicated fast electron transport through these electrodes from the electrolyte towards ITO surface. The magnitude of this current increased up to [IL]=2% (w/v) in case of Ag-C8/ITO and then decreased for [IL]> 2% (w/v) which may be attributed to the reduced mobility of ions (or electrons) caused by the hindrance occurring due to presence of long alkyl chains (C8). It is indicated that at higher [IL] concentration, some type of complex network formation took place. The alkyl chain length of ILs significantly affects the transport properties of the redox species at high concentrations, its effect on the redox potential should be minimal due the lack of a strong electron withdrawing or donating effect of alkyl groups [35]. However, in case of Ag-C2/ITO electrode maximum current was obtained for [IL]= 4% (w/v) indicating that the fast electron transport contributed to this gain and formation of complex network at higher [IL] concentration could not sustain the aforesaid mechanism. It can be seen that the Ag-C8/ITO electrode (curve b) shows higher magnitude of current (about double, 0.24 mA) as compared to Ag-C2/ITO (0.12 mA; curve d) electrode, and the bare ITO (curve a). These results indicatedAg-C8/ITO electrode exhibited preferentially higher electrocatalytic behaviour compared to Ag-C2/ITO electrode. This may be attributed to the formation of porous agar network permeable to redox species and Cl^- ions present in IL that contributed to electrode current. We can argue that the long alkyl chain of IL at low concentration enhanced the fast electron transfer from solution to electrode surface much faster as compared to the short alkyl chain IL molecule at higher concentration.

Figure 3 A

On the basis of the above mentioned observation, Ag-C8/ITO electrode with 2% (w/v) IL concentration and Ag-C2/ITO electrode consisting 4% (w/v) IL concentration was selected for fabrication of glucose biosensing electrode. These electrodes were used for immobilization of GOx for glucose detection. The magnitude of anodic peak current was significantly reduced (83.45 μA) after immobilization of GOx onto Ag-C8/ITO electrode (242.2 μA) due to insulating nature of enzyme [Figure 3A (c)]. It appears that GOx layer acted as a barrier for the electron transfer between the electrode surface and the redox probes in the solution. These results

confirmed immobilization of GOx onto Ag-C8/ITO electrode. It also suggested that Ag-C8/ITO bioelectrode provided a biocompatible environment. Where in case of Ag-C2/ITO electrode no significant change in anodic peak current was noticed (119.6 < 121.9 μA for Ag-C2/ITO electrode and GOx/Ag-C2/ITO, [Figure 3A (d & e)] respectively, but marginal potential shift towards positive side. This displacement of the potential toward higher values may be due to withdrawing effect of the imidazolium ring [35], indicating that negative charge on GOx electrostatically interacts with the positive charge on imidazolium ring.

Figure 3 B

The electrochemical studies of GOx/Ag-C8/ITO bioelectrode and GOx/Ag-C2/ITO bioelectrode were observed as a function of different scan rate. It was observed that in both bioelectrodes the magnitude of both anodic (I_{pa}) and cathodic (I_{pc}) peak currents increased linearly with square root of the scan rate ($v^{1/2}$), suggesting that electrochemical reaction was a diffusion-controlled process. Figure (3B) shows the cyclic voltammogram of GOx/Ag-C8/ITO bioelectrode with varying scan rate from 10 to100 mV/s.

The anodic (E_{pa}) and cathodic (E_{pc}) peak potentials and potential peak shifts ($\Delta E_p = E_{pa} - E_{pc}$) of GOx/Ag-C8/ITO electrode was observed to exhibit a linear relationship (linear regression coefficient 0.94) with the scan rate indicating facile charge transfer kinetics in the scan rate range from 10–100 mV s^{-1} in PBS containing 3.3 mM $[Fe(CN)_6]^{3-/4-}$ [Figure (3C)]. These results revealed that GOx/Ag-C8/ITO electrode provide sufficient accessibility to electrons between the electrolyte and the electrode. The diffusion co-efficient value of the redox species from the electrolyte to Ag/ITO, Ag-C8/ITO, GOx/Ag-C8/ITO, Ag-C2/ITO and GOx/Ag-C2/ITO bioelectrode was calculated using the Randles–Sevcik equation [36] as shown in Table 1. The higher D value was obtained for Ag-C8/ITO 5.9×10^{-11} cm^2 s^{-1} as compared to Ag-C2/ITO electrode indicates fast diffusion of redox species take place. The peak current I_p can be expressed as

$$I_p = (2.69 \times 10^5) n^{3/2} A D^{1/2} C v^{1/2} \quad \text{.....(1)}$$

where Ip is the peak current of the GOx/Ag-C8/ITO electrode (Ipa anodic and Ipc cathodic), n is the number of electrons involved or electron stoichiometry, A is the surface area of the electrode

($0.25\ cm^2$), D is the diffusion co-efficient, C is the concentration of redox species {3.3mM $[Fe(CN)_6]^{3/4}$} and v is the scan rate (20 mV s^{-1}).

The electroactive surface area (Ae) of the GOx/Ag-C8/ITO and GOx/Ag-C2/ITO bioelectrode is determined from the calculated diffusion co-efficient and the Randles–Sevcik equation [36].

$$A_e = S/(2.99 \times 10^5)n^{3/2}CD^{1/2} \quad \text{..... (2)}$$

where S is the slope of the straight line obtained from the graph of Ip versus scan rate $^{1/2}$. The Ae value of the GOx/Ag-C8/ITO and GOx/Ag-C2/ITO bioelectrode has been found to be 6.37 and 6.6 mm^2, respectively. These results indicate that more active surface area obtained at Ag-C2/ITO electrode.

The values of the slope, intercept and correlation coefficient of GOx/Ag-C8/ITO, and GOx/Ag-C2/ITO bioelectrodes are given in following Eqs. (3) to (6).

$$I_{pa}(A)_{GOx/Ag-C8/ITO} = 16.86\ \mu A + 7.7\ (\mu A\ mV/s)^{1/2}\ [\text{scanrate}\ (mV/s)]^{\frac{1}{2}}\ \text{with}R^2 = 0.99 \text{ ... ...} \quad (3)$$

$$I_{pc}(A)_{GOx/Ag-C8/ITO} = -11.32\ \mu A - 30.61\ (\mu A\ mV/s)^{1/2}\ [\text{scanrate}\ (mV/s)]^{1/2}\ \text{with}R^2 = 0.99 \text{ ....} \quad (4)$$

$$I_{pa}(A)_{GOx/Ag-C2/ITO} = 25.57\ \mu A + 7.52\ (\mu A\ mV/s)^{1/2}\ [\text{scanrate}\ (mV/s)]^{\frac{1}{2}}\ \text{with}R^2 = 0.99 \text{ ... ...} \quad (5)$$

$$I_{pc}(A)_{GOx/Ag-C2/ITO} = -16.36\ \mu A - 43.9\ (\mu A\ mV/s)^{1/2}\ [\text{scanrate}\ (mV/s)]^{1/2}\ \text{with}R^2 = 0.98 \text{ ....} \quad (6)$$

The surface concentration of ionic species of these electrodes was estimated using Brown–Anson model [36].

$$Ip = \frac{n^2F^2I^*AV}{4RT} \quad \text{..... (7)}$$

Where n is the number of electrons transferred which is 1 in this case, F is Faraday constant (96485.34 C mol^{-1}), A is surface area of the electrode ($0.25\ cm^2$), R is gas constant, I* is surface concentration of ionic species of electrode (mol/cm^2), T is 298 K, and I_p/V is the slope of calibration plot (scan rate value). The surface concentration of Ag-C8/ITO, GOx/Ag-C8/ITO, Ag-C2/ITO, and GOx/Ag-C2/ITO, bioelectrode was found to be 5.13×10^{-8} M/cm^2, 1.8×10^{-8} M/cm^2, 2.54×10^{-8} M/cm^2 and 2.6×10^{-8} M/cm^2 respectively. The results indicate that Ag-C8/ITO and Ag-C2/ITO electrode provides increased electroactive surface area for loading of enzymes (GOx). However, after the immobilization of GOx, the surface concentration changed, confirms the presence of GOx onto Ag-C8/ITO and Ag-C2/ITO electrodes surface with multilayer coverage. The surface concentration of GOx/Ag-C8/ITO and GOx/Ag-C2/ITO

bioelectrode was higher than the reported in literature [37], suggesting more GOx was immobilized on electrode surface.

Figure 3 C

The value of the heterogeneous electron transfer rate constant (K_s) obtained for Ag-C8/ITO, GOx/Ag-C8/ITO, Ag-C2/ITO, and GOx/Ag-C2/ITO bioelectrode was estimated to be 0.15, 0.11, 0.11 and 0.11 s^{-1} according to the model of Laviron as in eq. (8) [38].

$$K_s = mnFv/RT \quad (8)$$

Where m is the peak-to-peak separation (0.188, 0.145, 0.136, 0.139 V, respectively), F is the Faraday constant, v is the scan rate (20 mV s^{-1}), n is the number of transferred electrons (1), R is the gas constant and T is room temperature (25^0C). The highest value of K_s was found in case of Ag-C8/ITO electrode as compared to Ag-C2/ITO, GOx/Ag-C2/ITO and GOx/Ag-C8/ITO bioelectrodes, which indicated fast electron transfer between the electrode and electrolyte due to the presence of long alkyl chain of IL into matrix and higher than the previous reported as 0.030 s^{-1} for Au-poly[C10VIm$^+$][Cl$^-$] [18]. The changes in K_s also indicate that the adsorption of GOx onto Ag-C8/ITO electrode and Ag-C2/ITO electrode. Table 1 shows the electrochemical parameters obtained for different electrodes including Ag-C8/ITO, GOx/Ag-C8/ITO bioelectrode, Ag-C2/ITO and GOx/Ag-C2/ITO bioelectrode.

Table 1

Impedance Spectroscopy Studies

Electrochemical impedance technique is an efficient, versatile tool for investigating the interfacial properties of layer formation due to bio molecules and electrode interaction. The transport of electrochemically produced charge can be modelled by capacitance/resistance changes occurring at the electrode/electrolyte interface of modified surface. EIS spectra of bare ITO, Ag-C8/ITO, Ag-C2/ITO, GOx/Ag-C8/ITO and GOx/Ag-C2/ITO electrode has studied in PBS containing 3.3 mM $[Fe(CN)_6]^{3-/4-}$ to monitor charge transfer resistance (R_{CT}) at the electrode and electrolyte interface. Figure 4 demonstrates the faradic impedance spectra, presented as Nyquist plots obtained from real (Z') and imaginary ($-Z''$) in the frequency range 0.01–10^5 Hz at zero potential. The semicircle part corresponds to electron-transfer limited process and its

diameter is equal to the electron transfer resistance, R_{CT} that controls electron transfer kinetics of the redox probe at the electrode interface. The values of R_{CT} derived from the diameter of semicircle of impedance spectra are obtained as 7.33 kΩ for bare ITO (curve a), 5.85 kΩ for Ag-C8/ITO (curve b), 5.8 kΩ for GOx/Ag-C8/ITO (curve c) electrode, 6.36 kΩ for Ag-C2/ITO (curve d), and 5.2 Ω for GOx/Ag-C2/ITO (curve e) electrode. The semicircle of ITO (curve a) exhibits charge transfer phenomena between electrode and medium. Compared to bare ITO, R_{CT} value obtained for Ag-C8/ITO electrode and Ag-C2/ITO (curve b, d) decreases resulting in enhanced electron transfer or conductive pathway towards electrode. This suggests that presence of ILs and polyanionic agar enhance ionic transport in Ag-C8/ITO electrode results in the formation of complex and improved charge transfer. These results are in good agreement with the results of CV studies. It is found that the R_{CT} value obtained for the electrodes after GOx immobilization decreases, indicating successful modification of the Ag-C8/ITO and Ag-C2/ITO electrodes. These electrodes have been characterized by analyzing the parameters such as HET (k_e) and time constant τ. The value of R_{CT} is depend on electrochemical reaction time constant, τ ($1/2\pi f_{max} = R_{CT} \cdot Cp$, where f_{max} is the frequency at which maximum Z'' obtained, R_{CT} is the charge transfer resistance and Cp is the double layer capacitance) [39]. The corresponding k_e vale can be obtained by using eq. (9). Table 2 shows the EIS values obtained for respective electrodes.

$$k_e = RT/n^2F^2AR_{ct}C \quad \text{.....(9)}$$

The ionic conductivity of Ag-C8/ITO, Ag-C2/ITO electrode deduced from the Rs values by employing the formula σ =l/Rs A, where l is the thickness of electrode and A is the contact area between the electrode and electrolyte. The conductivity of Ag-C8/ITO and Ag-C2/ITO electrode found as 4.7 m s/cm and 6.6 m s/cm, respectively, which is highest for shorter side alkyl chain and it decrease with the increase in alkyl chain length as expected from larger van der Waals interactions. Thus, present results is in good agreement with Gelinas et al. where they reported that the conductivity of the ionic liquids varies with alkyl chain in 1-(methylferrocenyl)-3-methylimidazolium (FcEImC1) and 1-(methylferrocenyl)-3-dodecenylimidazolium (FcEImC12) conductivity found as 0.10 mS cm^{-1} and 0.04 mS cm^{-1}, respectively higher for shorter side alkyl chain and decrease with increase alkyl chain. The ionic conductivity of Ag-C8/ITO, Ag-C2/ITO electrode is higher than the reported in literature [35].

Table 2

Figure 4

Electrochemical response studies: The cyclic voltammetric (CV) studies were carried out to investigate the activity of the GOx/Ag-C8/ITO and GOx/Ag-C2/ITO bioelectrode as a function of glucose concentration (0.27-22.2 mM) at scan rate of 20 mV s^{-1} in PBS containing 3.3 mM $[Fe(CN)_6]^{3-/4-}$. It was observed that the magnitude of current increased with the glucose concentration as shown in Figure 5. The biochemical reaction taking place at electrode surface permits electrons to be directly accepted from the reduced GOx molecules in the presence of redox species (Med) as the mediator $[Fe(CN)_6]^{3-/4-}$. Moreover, the generated electrons shuttle (carried) by mediator from FAD center of GOx enzyme towards electrode followed the second generation of biosensor. Beside this, the generated electrons during the re-oxidation of GOx after enzymatic reaction are transferred to the Ag-C8/ITO and Ag-C2/ITO *via* redox couples resulting in enhanced charge transfer rate leading to increases magnitude of current. Moreover, we can say that $[Fe(CN)_6]^{3-/4-}$ moieties in the GOx/Ag-C8/ITO and GOx/Ag-C2/ITO bioelectrode act as electron donors in place of molecular oxygen for GOx and electron shuttles between GOx and the substrate ITO.

$$\text{Glucose} + O_2 \xrightarrow{GOx_{(oxi)}} \text{Gluconic acid} + H_2O_2 + GOx_{(red)} \quad \ldots\ldots\ldots\ldots\ldots\ldots \quad (10)$$

$$GOx_{(red)} + Med_{(oxi)} \xrightarrow{\text{e- shuttling}} Med_{(red)} + GOx_{(oxi)} + H^+ \quad \ldots\ldots\ldots\ldots\ldots\ldots \quad (11)$$

$$Med_{(red)} \longrightarrow M_{(oxi)} + e^- \text{ (at electrode)} \quad \ldots\ldots\ldots\ldots\ldots\ldots \quad (12)$$

Where, Med (oxi) and Med (red) are the oxidized and reduced forms of the mediator. The reduced form is reoxidized at the electrode, giving a current signal (proportional to the glucose concentration) while regenerating the oxidized form of the mediator.

With the increasing glucose concentration, the response current of GOx/Ag-C8/ITO and GOx/Ag-C2/ITO bioelectrode exhibit detection range from 0.27-22.2 mM but a good linear relationship in the ranges of 0.28-16.7 and 0.28-5.6 mM, respectively. The Michaelis–Menten constant K_m value was determined from the analysis of the slope and intercept for the plot of the reciprocals of current versus glucose concentrations, i.e., Lineweaver–Burke plot of 1/*I* versus 1/[glucose][40]. To reveal the affinity of the enzyme (GOx) for the analyte glucose, enzyme substrate kinetics parameters were probed. The value of apparent Michaelis–Menten constant (K_m) for GOx/Ag-C8/ITO and GOx/Ag-C2/ITO bioelectrodes was found as 0.023 mM and

0.0007 mM respectively. This low value K_m indicated that the higher affinity of GOx/Ag-C8/ITO and GOx/Ag-C2/ITO bioelectrodes towards glucose. The determined K_m is 0.023 and 0.0007 mM, a value considerably smaller than that reported for GOx in solution (22 mM) [41], and other GOx biosensor electrodes as Au/poly-3-(3-N,N-diethylaminopropoxyl) thiophene-SWNT composites [42], Au-poly[C10VIm$^+$][Cl$^-$] [18]. These GOx/Ag-C8/ITO and GOx/Ag-C2/ITO bioelectrode exhibited detection in the range 0.27-22.2 mM but good linearity obtained from 0.28-16.7 and 0.28-5.6 mM with sensitivity 4.0 $\mu AmM^{-1}cm^{-2}$ and 14.6 $\mu AmM^{-1}cm^{-2}$, respectively, which is higher than the reported in literature [16,18,43; Table 3]. The biosensing characteristics of GOx/Ag-C8/ITO and GOx/Ag-C2/ITO bioelectrode along with those reported in literature are summarized in Table 3.

Table 3

Figure 5

Determination of glucose concentration in human serum samples: Serum samples were collected from nearby hospital. These Serum samples were tested in order to demonstrate the practical usage of the GOx/Ag-C8/ITO and GOx/Ag-C2/ITO bioelectrode. The obtained results were summarized in Table 4. As we can see, the glucose values measured by the present system and given by hospital (auto analyzer) are very close. The result demonstrated good accuracy for the glucose sensing in real samples, ascertaining the practical application of the proposed glucose biosensor in clinical analysis. It has been observed that the GOx/Ag-C8/ITO electrode exhibit more accuracy with serum sample as compared to GOx/Ag-C2/ITO electrode due to its high electrocatalytic activity.

Table 4

The selectivity of GOx/Ag-C8/ITO and GOx/Ag-C2/ITO bioelectrode monitored using potential interferents such as ascorbic acid (AA), urea (U), cholesterol (Ch), oxalic acid (OA) has been monitored to evaluate selectivity of bioelectrode (Figure 6). The interferents solution were at normal concentration as glucose (5.0mM), citric acid (CA; 4.0mM), ascorbic acid (AA; 0.1mM), urea (U;1.0mM), oxalic acid and (OA;4.0mM), cholesterol (Ch;5.0mM) the electrochemical behaviour monitored under similar conditions using CV technique. The change in the oxidation peak was measured in PBS containing 3.3 mM $[Fe(CN)_6]^{3-/4-}$ using equal amount of glucose (1:1)

and above mentioned interferents. We found that the present bioelectrode is specific to glucose and does not show a significant response except OA. It may be due to self-redox behaviour of OA.

Figure 6

The shelf-life of the GOx/Ag-C8/ITO and GOx/Ag-C2/ITO bioelectrode was investigated by measuring electrochemical current response in regular interval for one week for about 4 weeks. It was observed that bioelectrode retained about 90% of GOx activity even after 4 weeks of preparation when stored under refrigerated conditions (4 ^{0}C). Thus, bioelectrodes reveals good storage stability upto 4 weeks.

Conclusions

Here, we have introduced a novel matrix consisting of agar in optimized ionic liquid concentration(Ionogel, Ig) as 2% and 4% for [1-octyl-3-methyl imidazolium chloride [C8mim][Cl] and 1-ethyl-3-methyl imidazolium chloride [C2mim][Cl] for detection of glucose. The SEM images clearly exhibit that in both ILs ([C8mim][Cl] and [C2mim][Cl]), agar was uniformly and homogeneous dispersed and formed a well oriented and stable electrode for electrochemical studies. We have extensively studied the step wise modification in fabrication of ionogel (Ag-C8/ITO, Ag-C2/ITO) electrode and their loading of GOx with electrochemical techniques (cyclic voltammetry). It has been observed that the GOx/Ag-C8/ITO electrode provide high electrocatalytic activity that achieved broad detection range of glucose (0.277-22.2 mM). However, the higher sensitivity (14 μA mM^{-1} cm^{-2}) and low value of K_m (0.0007 mM) obtained with GOx/Ag-C2/ITO electrode as a function of glucose detection. It was found that the ILs consisted of diverse properties that could be utilized for design of other point of care diagnostics devices.

Acknowledgement

AS acknowledges University Grants Commission, Government of India for a research fellowship. This work was supported by a grant received from Department of Science and Technology, Government of India (grant no.SB/PC/S1/110/2012). Authors are thankful to the Advanced Instrument Research Facility of the University for providing access to FTIR and SEM instruments.

References

[1] J.L. Bideau, L. Viaub, A. Vioux, Ionogels, ionic liquid based hybrid material, Chem. Soc. Rev. 40 (2011) 907-925.

[2] Y. He, T.P. Lodge, A thermoreversible ion gel by triblock copolymer self-assembly in an ionic liquid, Chem. Commun. (2007) 2732-2734.

[3] Y. Lei, T.P. Lodge, Effects of component molecular weight on the viscoelastic properties of thermoreversible supramolecular ion gels via hydrogen bonding, Soft Matter 8 (2012) 2110-2120.

[4] M. Kofu, T. Someya, S. Tatsumi, K. Ueno, T. Ueki, M. Watanabe, T. Matsunaga, M. Shibayama, V.G. Sakai, M. Tyagi, O. Yamamuro, Microscopic insights into ion gel dynamics using neutron spectroscopy, Soft Matter 8 (2012) 7888-7897.

[5] J.F. Stanzione, R.E. Jensen, P.J. Costanzo, G.R. Palmese, Synthesis and characterization of ionic polymer networks in a room-temperature ionic liquid. ACS Appl. Mater Interfaces 4 (2012) 6142-6150.

[6] J.C. Ribot, C. Guerrero-Sanchez, R. Hoogenbooma, U.S. Schubert, Aqueous gelation of ionic liquids: reverse thermoresponsive ion gels, Chem. Commun. 46 (2010) 6971–6973.

[7] R.P. Swatloski, S.K. Spear, J.D. Holbrey, R.D. Rogers, Dissolution of Cellose with Ionic Liquids, J. Am. Chem. Soc. 124 (2002) 4974-4975.

[8] S. Tan, D. Macfarlane, Ionic liquids in biomass processing, in: Ionic Liquids, B. Kirchner (Eds.), Springer, Germany, 2010, pp. 311-340.

[9] K. Rawat, H.B. Bohidar, Universal charge quenching and stability of proteins in 1-methyl-3-alkyl (hexyl/octyl) imidazolium chloride ionic liquid solutions, J. Phys. Chem. B 116 (2012) 11065−11074.

[10] K. Ueno, M. Watanabe, From colloidal stability in ionic liquids to advanced soft materials using unique media, Langmuir 27 (2011) 9105-9115.

[11] J.M.E. Pusch, D. Brondani, L. Luza, J. Dupont, I.C. Vieira, Pt-Pd bimetallic nanoparticles dispersed in an ionic liquid and peroxidase immobilized on nanoclay applied in the development of a biosensor, Analyst 138 (2013) 4898.

[12] H.Y. Xiong, T. Chen, X.H. Zhang, S.F. Wang, High performance and stability of a hemoglobin-biosensor based on an ionic liquid as nonaqueous media for hydrogen peroxide monitoring, Electrochem. Commun. 9 (11) (2007) 2671-2675.

[13] M.K. Gupta, S.K. Khokhar, D.M. Phillips et al, Patterned silk films cast from ionic liquid solubilized fibroin as scaffolds for cell growth, Langmuir, 23(3) (2007) 1315-1319.

[14] M.M. Musameh, R.T. Kachoosangi, L. Xiao, A .Russell, R.G. Compton, Ionic liquid-carbon composite glucose biosensor, Biosens. Bioelectron. 24 (2008) 87-92.

[15] W. Wang, G. Yin, X. Ma, J. Wan, Simple method for preparing glucose biosensor based on glucose oxidase in nanocomposite material of single-wall carbon nanotubes/ionic liquid, J. Anal. Sci. Meth. Instrument. 2 (2012) 54-59.

[16] B. Haghighi, R. Nikzad, Prussian blue modified carbon ionic liquid electrode: electrochemical characterization and its application for hydrogen peroxide and glucose measurements, Electroanalysis, 21 (16) (2009) 1862-1868.

[17] D. Ragupathy, A.I. Gopalan, K.P. Lee, Synergistic contributions of multiwall carbon nanotubes and gold nanoparticles in a chitosan–ionic liquid matrix towards improved performance for a glucose sensor, Electrochem. Communi. 11(2009) 397-401.

[18] S. Lee, B.S. Ringstrand, D.A. Stone, M.A. Firestone, Electrochemical activity of glucose oxidase on a poly(ionic liquid)–Au nanoparticle composite, ACS Appl. Mater Interfaces, 4 (2012) 2311-2317.

[19] K.V. Ozdokur, B. Demir, E. Yavuz, F. Ulus, C.E. Aydın, D.O. Demirkol, L. Pelit, S. Timur, F.N. Ertas, Pyranose oxidase and Pt–MnO_x bionanocomposite electrode bridged by ionic liquid for biosensing applications, Sens. Actuat. B, 197 (2014) 123-128.

[20] N.M.T. Lourenco, J. Osterreicher, P. Vidinha, S. Barreiros, C.A.M. Afonso, J.M.S. Cabral, L.P. Fonseca, Effect of gelatine ionic-liquid functional polymers on glucose oxidase and horseradish peroxidise kinetics, React. Funt. Poly. 71 (2011) 489-495.

[21] P.R. Solanki, A. Kaushik, V.V. Agrawal, B.D. Malhotra, Nanostructured metal oxide-based biosensors, NPG Asia Mater, 3 (2011) 17-24.

[22] Z. Li, H. Liu, Y. Liu, P. He, J. Li, A room-temperature ionic-liquid-templated proton-conducting gelatinous electrolyte, J. Phys. Chem. B, 108 (2004) 17512.

[23] M.A. Neouze, J.L. Bideau, F. Leroux, A. Vioux, A route to heat resistant solid membranes with performances of liquid electrolytes, Chem. Commun. (2005)1082-1084.

[24] P. Wang, S.M. Zakeeruddin, P. Comte, I. Exnar, M. Gratzel, Gelation of ionic liquid-based electrolytes with silica nanoparticles for quasi-solid-state dye-sensitized solar cells, J. Am. Chem. Soc. 125 (2003) 1166.

[25] A. Hayashi, M. Yoshizawa, C.A. Angell, F. Mizuno, T. Minami, M. Tatsumisago, High conductivity of superionic-glass-in-ionic-liquid solutions, Electrochem. Solid State Lett. **6**(8) (2003) E19-E22.

[26] S. Yamazaki, A. Takegawa, Y. Kaneko, J. Kadokawa, M. Yamagata, M. Vlshikawa, An acidic cellulose–chitin hybrid gel as novel electrolyte for an electric double layer capacitor, Electrochem. Commun. 11(2009) 68-70.

[27] N. Winterton, Solubilization of polymers by ionic liquids, J. Mater. Chem. 16 (2006) 4281-4293.

[28] J.L. Bideau, L. Viaub, A. Vioux, Ionogels, ionic liquid based hybrid materials, Chem. Soc. Rev. 40 (2011) 907.

[29] J.S. Craigie, C. Leigh, J.A. Hellebust, J.S. Craigie, Carrageenans and agars, in: J.A. Hellebust, J.S. Caraigie (Eds.), Handbook of phycological methods, physiological and biochemical methods, Cambridge University Press, Cambridge, 1978, 109-131.

[30] S. Boral, H.B. Bohidar, Effect of water structure on gelation of agar in glycerol solutions and phase diagram of agar organogels, J. Phys. Chem. B, 116 (2012) 7113-21.

[31] M. Duckworth, W. Yaphe, The structure of agar: Part I. Fractionation of a complex mixture of polysaccharides, Carbohydrate Research, 16 (1971) 189-197.

[32] J.Y. Xiong, J. Narayanan, X.Y. Liu, T.K. Chong, S.B. Chen, T.S. Chung, Topology evolution and gelation mechanism of agarose gel, J. Phys. Chem. B 109 (2005) 5638-5643.

[33] D. Bulone, P.L. San Biagio, Microgel regions in dilute agarose solutions: the notion of non-gelling concentration, and the role of spinodal demixing, Chem. Phys. Letts. 179 (1991) 339.

[34] K. Prasad, A.K. Siddhanta, A.K. Rakshit, A. Bhattacharya, P.K. Ghosh, On the properties of agar gel containing ionic and non-ionic surfactants, Int. J. Biol. Macromolecules, 35 (2005) 135-144.

[35] B. Gelinas, J. C. Forgie, D. Rochefort, Conductivity and electrochemistry of ferrocenyl-imidazolium redox ionic liquids with different alkyl chain lengths, J. Electrochem. Soc. 161(4) (2014) H161-H165.

[36] A.J. Bard, L.R. Faulkner, Electrochemical Methods: Fundamentals and Applications, 2nd ed., New York: John Wiley & Sons, New York 1980.

[37] M. RongNa, W. Bin, L. Yan, L. Jing, Z. Qian, W.G. Tao, J.W. Li, W.H. Sheng, Direct electrochemistry of glucose oxidase on the hydroxyapatite/Nafion composite film modified electrode and its application for glucose biosensing, Sci. China Ser B-Chem. 52(11) (2009) 2013-2019.

[38] J. Singh, A. Roychoudhury, M. Srivastava, P.R. Solanki, D.W. Lee, S.H. Lee, B.D. Malhotra, A highly efficient rare earth metal oxide nanorods based platform for aflatoxin detection, J. Mater. Chem. B 1 (2013) 4493-4503.

[39] E. Laviron, General expression of the linear potential sweep voltammogram in the case of diffusionless electrochemical systems, J. Electroanal. Chem. 101 (1979) 19-28.

[40] P.R. Solanki, A. Kaushik, A.A. Ansari, A. Tiwari, B.D. Malhotra, Multi-walled carbon nanotubes/sol-gel derived silica/chitosan nanobiocomposite for total cholesterol sensor, Sens. Actuat. B Chem., 137 (2009) 727-735.

[40] B. Wang, B. Li, Q. Deng, S. Dong, Amperometric glucose biosensor based on organic/inorganic hybrid material, Anal. Chem. 70 (1998) 3170-3174.

[41] X. Pang, P. Imin, I. Zhitomirsky, A. Adronov, Amperometric detection of glucose using a conjugated polyelectrolyte complex with single-walled carbon nanotubes, Macromolecules, 43 (2010) 10376-10381.

[42] M.S.P. Lopez, D. Mecerreyes, E. Lopez-Cabarcos, B. Lopez-Ruiz, Amperometric glucose biosensor based on polymerized ionic liquid microparticles, Biosens. Bioelectron., 21(12) (2006) 2320-2328.

Figure Captions

Fig. 1 SEM images of (a) Ag-C8/ITO, (b) GOx/Ag-C8/ITO bioelectrode, (c)Ag-C2/ITO; (d) GOx/Ag-C2/ITO bioelectrodes.

Fig. 2. FTIR spectra of (a) Ag/ITO; (b) Ag-C8/ITO; (c) Ag-C2/ITO; (d) GOx/Ag-C8/ITO bioelectrodes.

Fig. 3(A). Cyclic voltammograms of (a) bare ITO; (b) Ag-C8/ITO electrode; (c) GOx/Ag-C8/ITO bioelectrode; (d) Ag-C2/ITO; (e) GOx/Ag-C2/ITO bioelectrode at scan rate of 20 mV/s in PBS containing 3.3 mM $[Fe(CN)_6]^{3-/4-}$. Inset shows the plot between current and varying percentage (0-5%) of [C8mim][Cl] and [C2mim][Cl] in agar based electrode onto ITO surface.

Fig. 3(B): Shows CV of GOx/Ag-C8/ITO bioelectrode as function of scan rate varying from 10 to 100 mV/s in PBS containing 3.3 mM $[Fe(CN)_6]^{3-/4-}$. Inset (a) and (b) shows the graph of current and potential Vs $\sqrt{\text{scan rate}}$ respectively.

Fig. 3(C): Shows E_{pa}, E_{pc} and ΔE_p of GOx/Ag-C8/ITO bioelectrode as a function of scan rate.

Fig. 4. Nyquist plot of (a) bare ITO electrode, (b) Ag-C8/ITO electrode, (c) GOx/Ag-C8/ITO electrode, (d) Ag-C2/ITO electrode, (e) GOx/Ag-C2/ITO electrode at zero potential in PBS containing 3.3 mM$[Fe(CN)_6]^{3-/4-}$ (inset: Randles equivalent circuit, where R_s: solution resistance, R_{CT}: charge transfer resistance, Z_w: Warburg impedence, and C_{dl}: double layer capacitance.

Fig. 5: Electrochemical response studies of GOx/Ag-C8/ITO bioelectrode; plot between current values Vs glucose concentration 5-400 mg/dl obtained from CV in PBS containing 3.3 mM $[Fe(CN)_6]^{3-/4-}$. Inset shows plot obtained from current values Vs glucose concentration with respect of GOx/Ag-C2/ITO bioelectrode.

Fig. 6: Selectivity studies of GOx/Ag-C2/ITO bioelectrode.

Table 1: Shows the electrochemical parameters: Anodic peak current (I_{pa}), Cathodic peak current (I_{pc}), Charge transfer rate constant (K_s) Diffusion coefficient (D), Electroactive surface area (Ae) Average surface concentration (Ae) for respective electrodes.

Table 2. Equivalent circuit elements of different fabricated electrodes.

Table 3: Some of ionic liquid containing glucose biosensor in the literature along with GOx/Ag-C8/ITO and GOx/Ag-C2/ITO bioelectrode.

Table 4: Determination of glucose in blood serum (n = 3) samples.

Figure 1

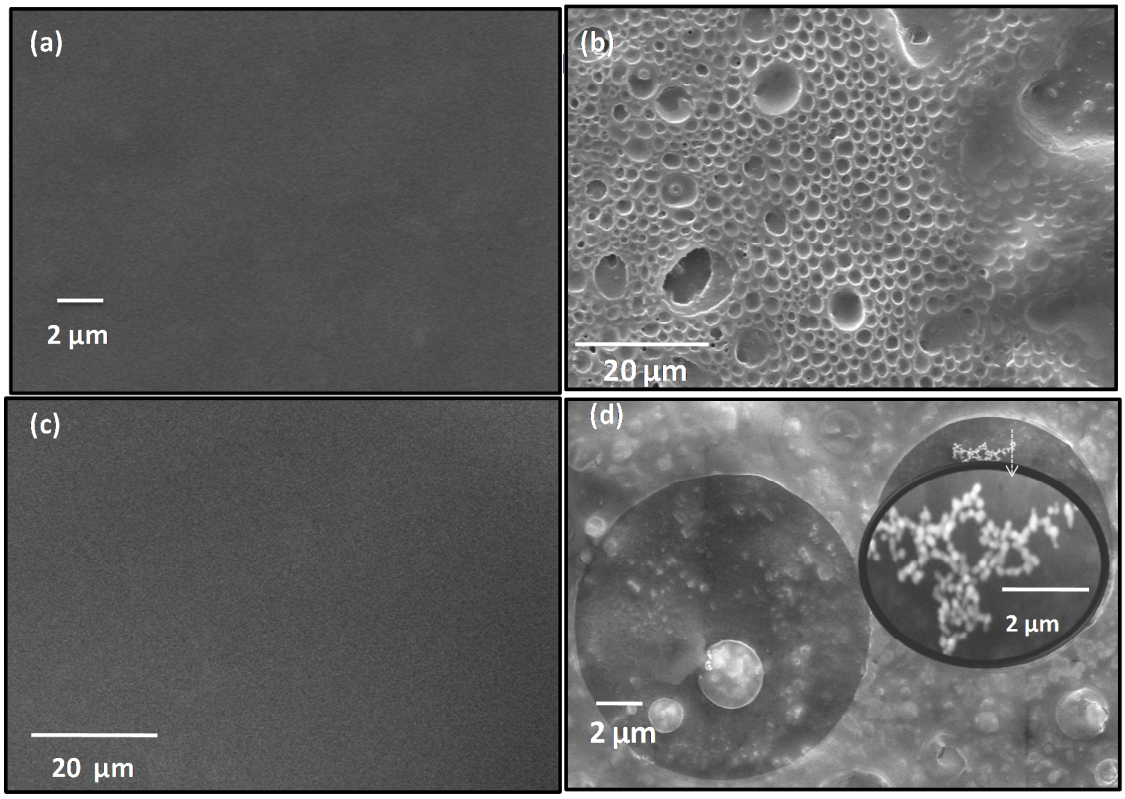

Figure 2

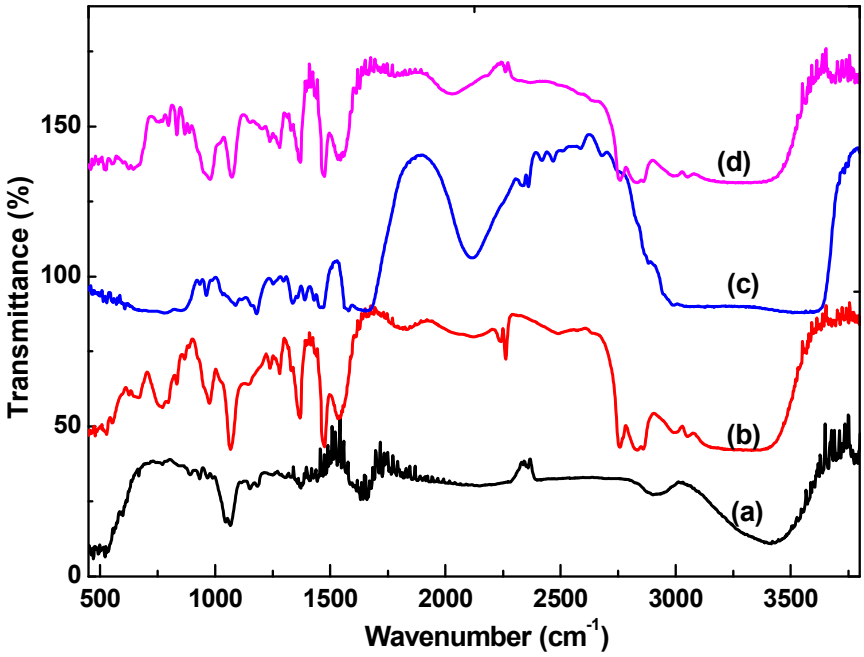

Figure 3(A)

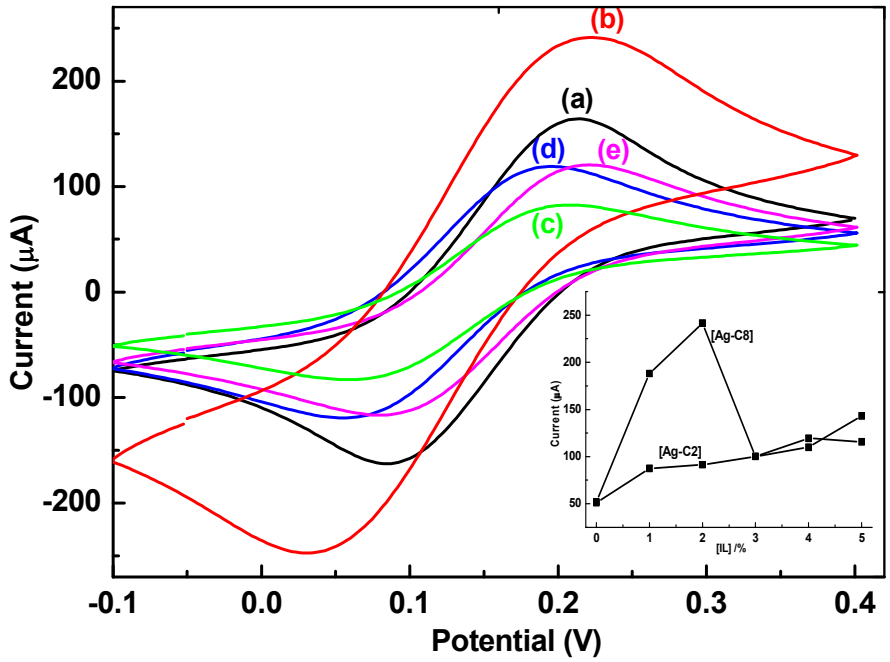

Figure 3(B)

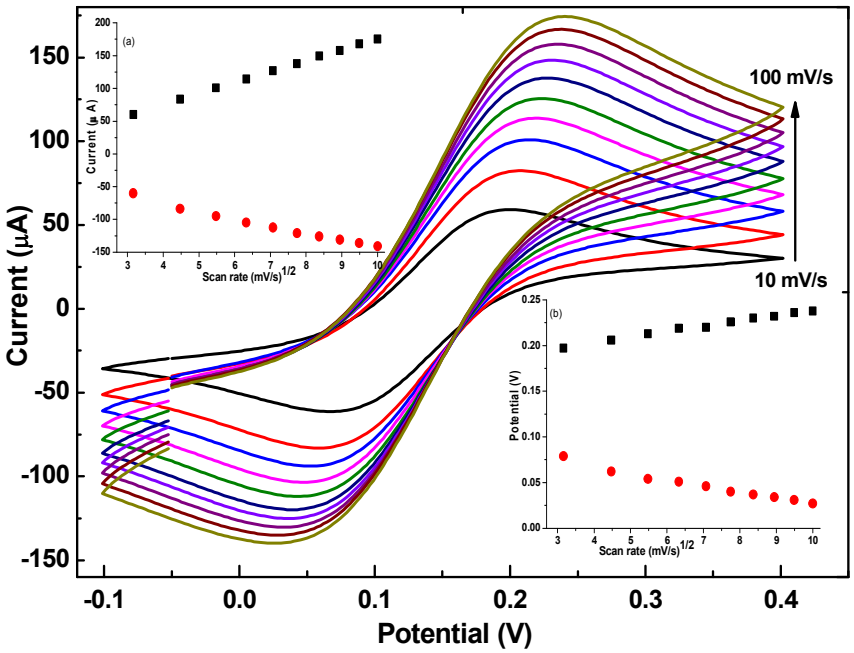

Figure 3(C)

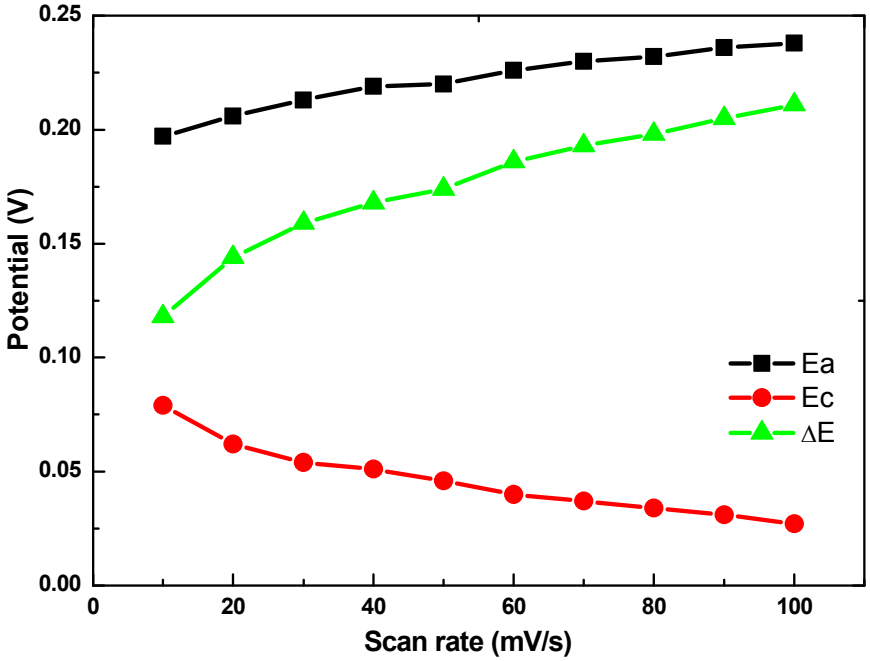

Figure 4

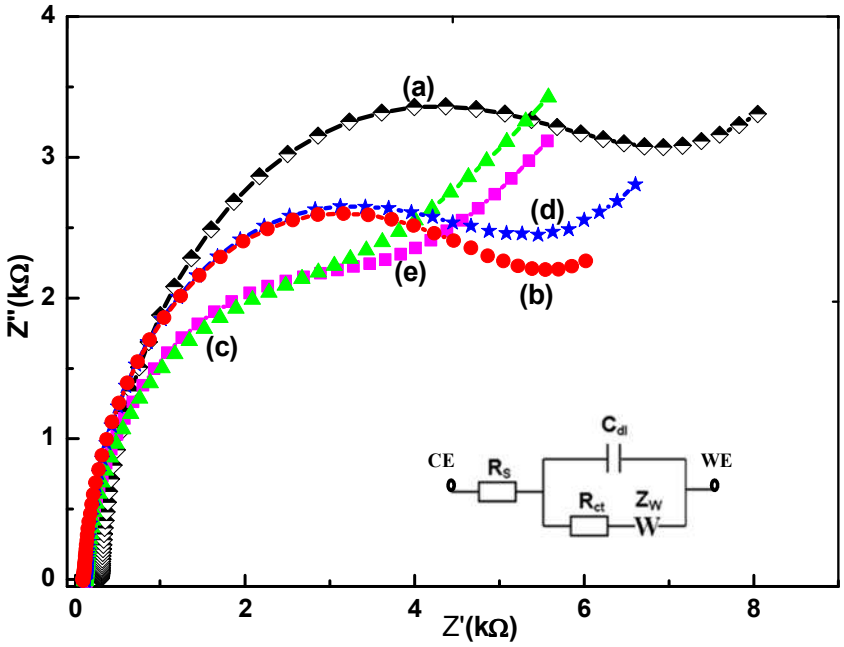

Figure 5

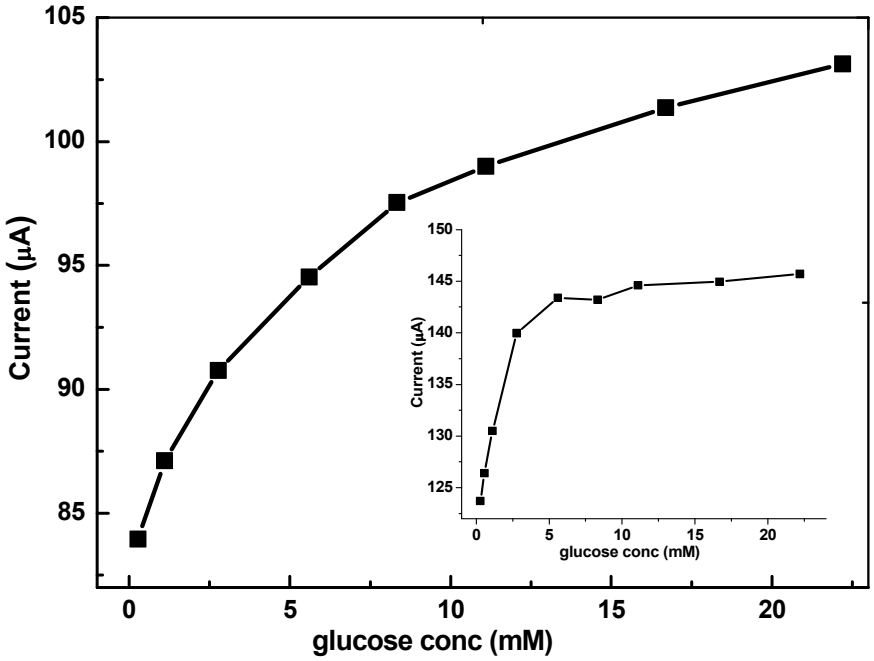

Figure 6

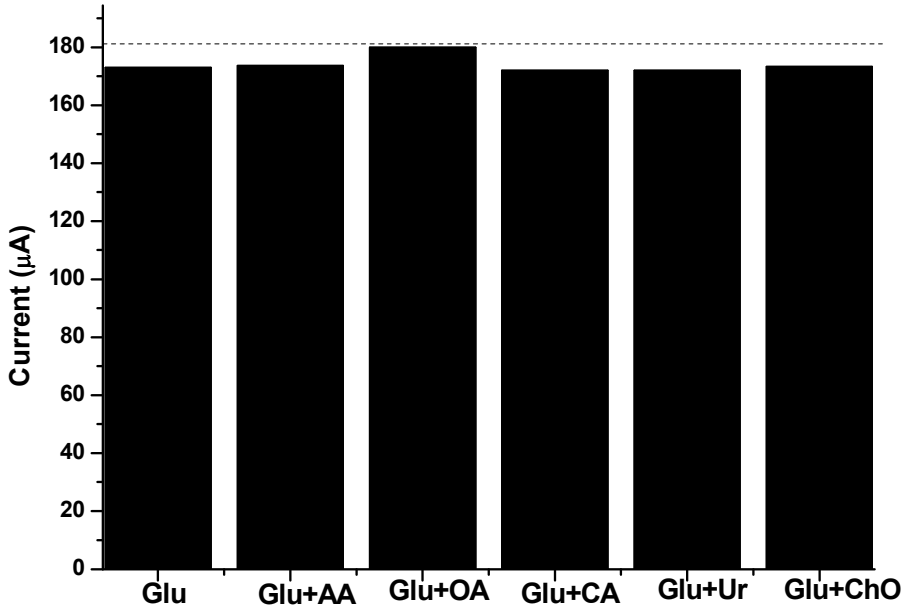

Table 1

Electrodes	I_{pa} (µA)	I_{pc} (µA)	K_s (s^{-1})	D (cm^2s^{-1})	Ae (mm^2)	I* (mol cm^{-2})
Ag-[C2]/ITO	119.6	-119.6	0.11	1.44×10^{-11}	7.02	2.54×10^{-8}
GOx/Ag-[C2]/ITO	121.9	-117	0.11	1.5×10^{-11}	6.6	2.6×10^{-8}
Ag-[C8]/ITO	242.2	-250.4	0.15	5.9×10^{-11}	5.57	5.13×10^{-8}
GOx/Ag-[C8]/ITO	83.45	-83.47	0.11	7×10^{-12}	6.37	1.8×10^{-8}

Table 2

EIS values	**Bare ITO**	**Ag-C8/ITO electrode**	**Ag-C2/ITO electrode**	**GOx/Ag-C8/ITO electrode**	**GOx/Ag-C2/ITO electrode**
R_{CT} (kΩ)	7.33	5.85	6.36	5.8	5.2
Rs(Ω)	298.2	93.92	67	58	109.4
Cp (µF)	2.64	3.6	2.84	4.8	3.82
n	0.99	0.99	0.99	0.99	0.99
τ (ms)	19.4	21	18	27.84	19.86
k_e (cm/s)	0.44×10^{-4}	0.55×10^{-4}	0.5×10^{-4}	0.56×10^{-4}	0.62×10^{-4}

Table 3

Electrode composition	**Linear range**	**Sensitivity (µAmM^{-1})**	**K_m** (mM)	**Stability**	**References**
GOx/IL/graphite(CPE)	2.0-20mM	-	-	-	[14]
GOx/nafion/SWCNTs-IL/GCE	0.5-12µM	-	-	-	[15]
cPB-CILEs/GOx-Nafion	0.001-2.0mM	1.9	-	-	[16]
GOx/Au/CS-IL-MWNT(SH)/ITO	1.0-10mM	4.1	-	3 weeks	[17]
Au NP-poly(IL)/GOx	-	0.093	1.23	-	[18]
PyOx-IL-Pt-MnOx/GCE	0.05-0.75mM	6.10	-	-	[19]
GOx/PILM/NF/Pt	0.07-8.0mM	0.64	-	150 days	[43]
GOx/Ag-[C8]/ITO	0.28-16.7mM	4.1	0.023	5 weeks	Present work
GOx/Ag-[C2]/ITO	0.28-5.6mM	14.6	0.0007	5 weeks	Present work

Table 4.

S.No.	Measured by Auto analyzer (Hitachi) available at hospital (mM)	Measured by developed biosensor (mM)	Bias (mM)	Measured by biosensor (mM)	Bias (mM)
	GOx/Ag-C8/ITO bioelectrode			GOx/Ag-C2/ITO bioelectrode	
1 Sample	5.70	5.90	+0.20	4.80	-0.90
2 Sample	6.06	6.20	+0.14	5.20	-0.86
3 Sample	7.92	7.80	-0.12	8.50	+0.58